NORSAR

NORSAR Scientific Report No. 2-2011

Semiannual Technical Summary

1 January - 30 June 2011

Frode Ringdal (ed.)

Kjeller, August 2011

6.4 The International Polar Year (IPY) broadband ocean-bottom seismograph deployment: observations, limitations and integration with the IPY land network

6.4.1 Introduction

Within the framework of the International Polar Year 2007-2008 (IPY) project "The Dynamic Continental Margin Between the Mid-Atlantic-Ridge System (Mohns Ridge, Knipovich Ridge) and Bear Island" (Schweitzer et al., 2008), several temporary seismic stations were installed in the wider area of the Western Barents Sea margin (Fig. 6.4.1). Among them was a three-component, broadband ocean-bottom seismometer and hydrophone (OBS/H) deployment, consisting of 12 stations distributed over the area between the Knipovich Ridge and Bear Island. Regarding land stations, the Norwegian National Seismic Network (NNSN) station HOPEN was upgraded with a broadband seismometer, a new broadband station (HSPB) was installed at Hornsund, and a small-aperture seismic array was installed on Bear Island for the summer season of 2008.

This network, together with the permanent stations in the wider region, was used to monitor and locate the seismicity around the continental margin and along the mid-ocean ridge, focusing on the sedimentary wedge between them. This contribution will mainly deal with a description of the seafloor network, its observations, and its integration with the land-based network in order to locate the seismicity in the target area.

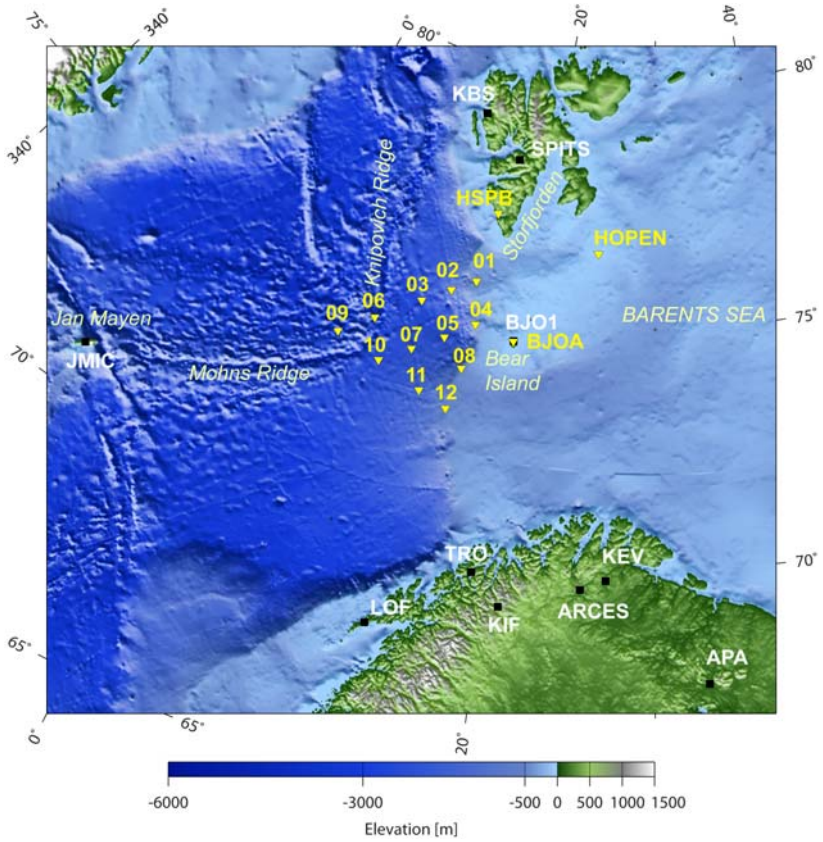

Fig. 6.4.1. Locations of seismic stations used within the IPY project. The IPY network is depicted in yellow, together with permanent seismic stations in the region, shown in black.

6.4.2 The IPY OBS/H deployment: instrumentation and data quality

The OBS/H stations were provided by the German Pool for Amphibian Seismology (DEPAS, www.awi.de/en/research/research_divisions/geosciences/geophysics/depas_german_instrument_pool_for_amphibian_seismology/), and were deployed by colleagues from the Alfred Wegener Institute, the University of Potsdam, KUM and the staff of the Polish research vessel HORYZONT II in late September 2007. The particular station model, known as LOBSTER (Longterm OBS for Tsunami and Earthquake Research), consists of a titanium frame that carries the broadband seismometer, recorder, releaser and batteries, each in a titanium pressure tube, as well as float units of syntactic foam, hydrophone, flasher, radio beacon and signal flag (Fig. 6.4.2). The seismometer is a CMG-40T by Güralp Systems Ltd. and the hydrophone is an HTI-04-PCA/ULF by High Tech Inc., USA, while data acquisition is performed by a GEOLON-MCS recorder in a Titanium tube, manufactured by SEND Off-Shore Electronics GmbH.

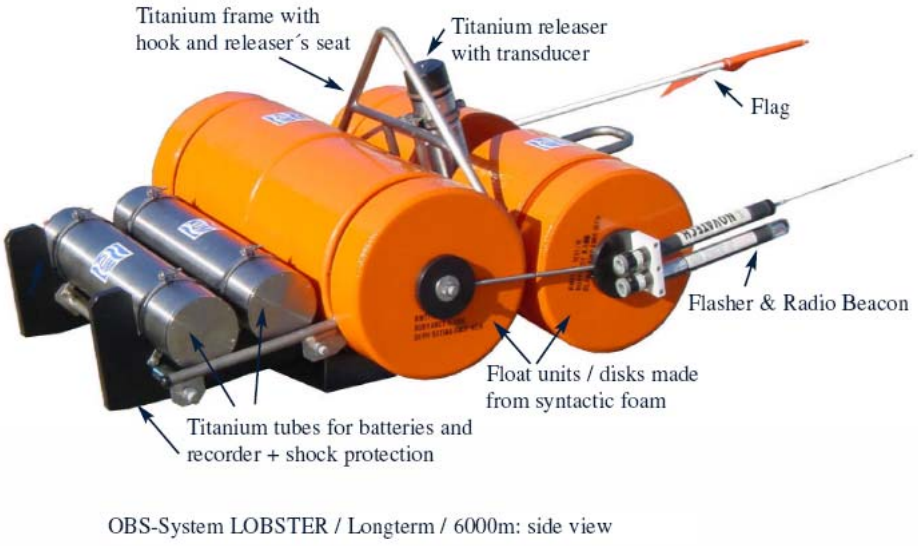

Fig. 6.4.2. The LOBSTER OBS/H system (picture taken from K.U.M. GmbH LOBSTER brochure).

The instrument response for the seismic channels was calculated, using information by the manufacturers of the sensors and data recorders (Güralp Systems, Ltd. and SEND Off-Shore Electronics GmbH, respectively). The pole-zero set for the CMG-40T is the following:

Table 6.4.1. Poles and zeroes of the Güralp CMG-40T seismometers of the DEPAS OBSs.

POLES (HZ)	ZEROES HZ
$-11.78 \times 10^{-3} \pm j11.78 \times 10^{-3}$	0
$-80.0 \pm j\ 95.0$	0

The normalizing factor at 1 Hz is A = 15.41 K. Sensitivity values are channel specific, a nominal value being about 2000 V/m/s.

The GEOLON-MCS recorder features software selectable pre-amplification, achievable in seven 6 dB steps, and which in the case of the OBS channels is set to GAIN = 1. This defines the sensitivity of the 24-bit A/D converter, based on the formula (SEND GmbH, 2009):

$$UIN_{0dB} = 5\ V\ /\ GAIN\ [Vpp\ differential]$$

Thus, the sensitivity is equal to 2x(5/1) Vfull-scale / 2^{24} = 0.59605 μV/bit.

Apart from the pre-amplifier, the GEOLON-MCS A/D converter consists of a sigma-delta modulator and a digital filter, which decimates down to the desired data sampling rate (SEND GmbH, 2007). The Cirrus Logic CS5378 low-power, single-channel, digital filter is used for this purpose (Cirrus Logic, 2010). A cascade of a multi-staged SINC filter with variable decimation stages and two FIR filters are employed to decimate from the 512 kHz of the modulator to a diversity of sampling rates. In the case of the IPY OBS/H deployment, 50 sps data was outputted. The employed digital filter cascade is the following:

FIR filter SINC-1, decimates by 8, symmetric, 36 coefficients: 512 kHz –> 64 kHz

FIR filter SINC-2-stage-2, decimates by 2, symmetric, 5 coefficients: 64 kHz –> 32 kHz

FIR filter SINC-2-stage-3, decimates by 2, symmetric, 6 coefficients: 32 kHz –> 16 kHz

FIR filter SINC-2-stage-4, decimates by 2, symmetric, 7 coefficients: 16 kHz –> 8 kHz

FIR filter SINC-3-stage-3, decimates by 5, symmetric, 17 coefficients: 8 kHz –> 1600 Hz

FIR filter SINC-3-stage-5, decimates by 2, symmetric, 6 coefficients: 1600 Hz –> 800 Hz

FIR filter SINC-3-stage-7, decimates by 2, symmetric, 7 coefficients: 800 Hz –> 400 Hz

FIR filter FIR1 (set 0), decimates by 4, symmetric, 48 coefficients: 400 Hz –> 100 Hz

FIR filter FIR2 (set 0), decimates by 2, symmetric, 126 coefficients: 100 Hz –> 50 Hz

As an example, the displacement amplitude and phase response for the vertical component of OBS01 is shown in Fig. 6.4.3. The shaded area notes the frequency range beyond the Nyquist (25 Hz).

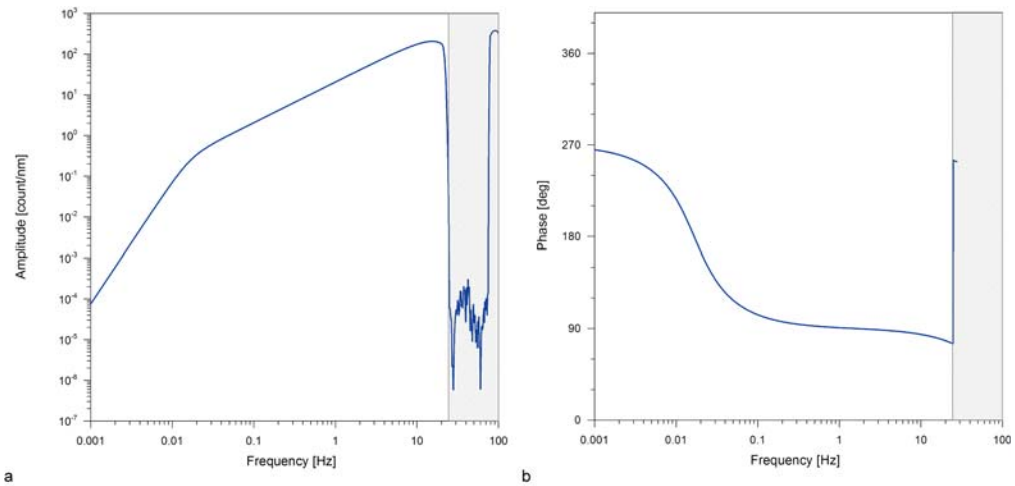

Fig. 6.4.3. a. Displacement amplitude response for the vertical, seismic channel of OBS01. b. Phase response for the same channel. The shaded area lies beyond the Nyquist frequency (25 Hz).

Regarding the response of the pressure sensor, only its gain is known, provided by the manufacturer in the brief documentation accompanying the shipped instruments (High Tech, Inc., 2005), a nominal value being equal to -195 dB relative to 1 V/μPa. A response curve is given in the same document, but without any information on how to reconstruct it.

The stations covered a wide variety of oceanic environments, from the shallow waters of the Barents Sea shelf (minimum depth 325 m for OBS01) to depths of about 2900 m close to the mid-ocean ridge (OBS09) and had a minimum inter-station distance of about 60 km. They were collected again in August 2008, after recording for a time interval of approximately 11 months. One of the shallowest stations (OBS04) was already fished out in April 2008 by a Russian trawler, while OBS03 was lost during recovery. OBS10 could not be recovered and was eventually found in April 2009 on the northern coast of Iceland, without having recorded data. Thus, there is partial data loss for OBS04 and total loss for OBS03 and OBS10.

Regarding the quality of the retrieved data, it mostly depends on additional possible problems, such as coupling conditions to the seafloor, low amplification etc., the possibility to apply the skew correction for timing, and the general noise conditions. Some problems were observed with particular seismometer components (vertical of OBS02, Y-component of OBS07, X-component of OBS12), while OBS02 had stopped recording a week before recovery, presumably due to problems with its power supply. This resulted in no skew correction for this station, as well as for the fished out station, OBS04. The rather frequent clipping of the horizontal components of OBS04 is suggestive of poor coupling to the seafloor, which may have been the reason that the station was fished out. No problems were detected on the hydrophone data.

Noise conditions are a very decisive factor affecting OBS/H data. The noise spectrum in the ocean is quite complex, with numerous sources contributing to it, including among others weather related phenomena, ocean currents, marine biologics and boat traffic (e.g., Wenz, 1962). In the case of the IPY OBS/H deployment, noise conditions were rather bad, extreme even in cases, with the shallower stations being worse. By far the best noise conditions were encountered at OBS09, the deepest station, close to the Mohns – Knipovich Ridge Bend, with second best being OBS06, also at a depth larger than 2300 m. The power spectral density plots of Figs. 6.4.4 and 6.4.5 show the average noise level (red line) at different stations for a period of one month (April 2008) and positive deviations from it (color scaled), for the OBS vertical component and the hydrophone, respectively. High noise conditions at all stations except for OBS09 can be observed in the typical seismic body-wave frequency range (1 – 10 Hz) in Fig. 6.4.4.

Comparing the same frequency range with Fig. 6.4.5, it becomes obvious that the hydrophones have lower noise levels, which has enabled in some cases the picking of first arrivals, when this was impossible on the seismic channels. A waveform example in Fig. 6.4.6 from the same time interval shows clearly the effect of poor signal-to-noise ratio (SNR) on the analysis of seismic events. The event occurred at the Mohns – Knipovich Bend (73.952°N, 8.819°E), on 27 April 2008, 23:49:52.6 UTC and waveforms are displayed sorted with epicentral distance and filtered between 3.5 and 12 Hz. Clear P-phase picks can be obtained on OBS06, OBS07 and OBS09, as well as the farther away OBS01, but not at in between distances. This is representative of how noise conditions affected the location capability of the network, taking also into account the quite small magnitude of most events.

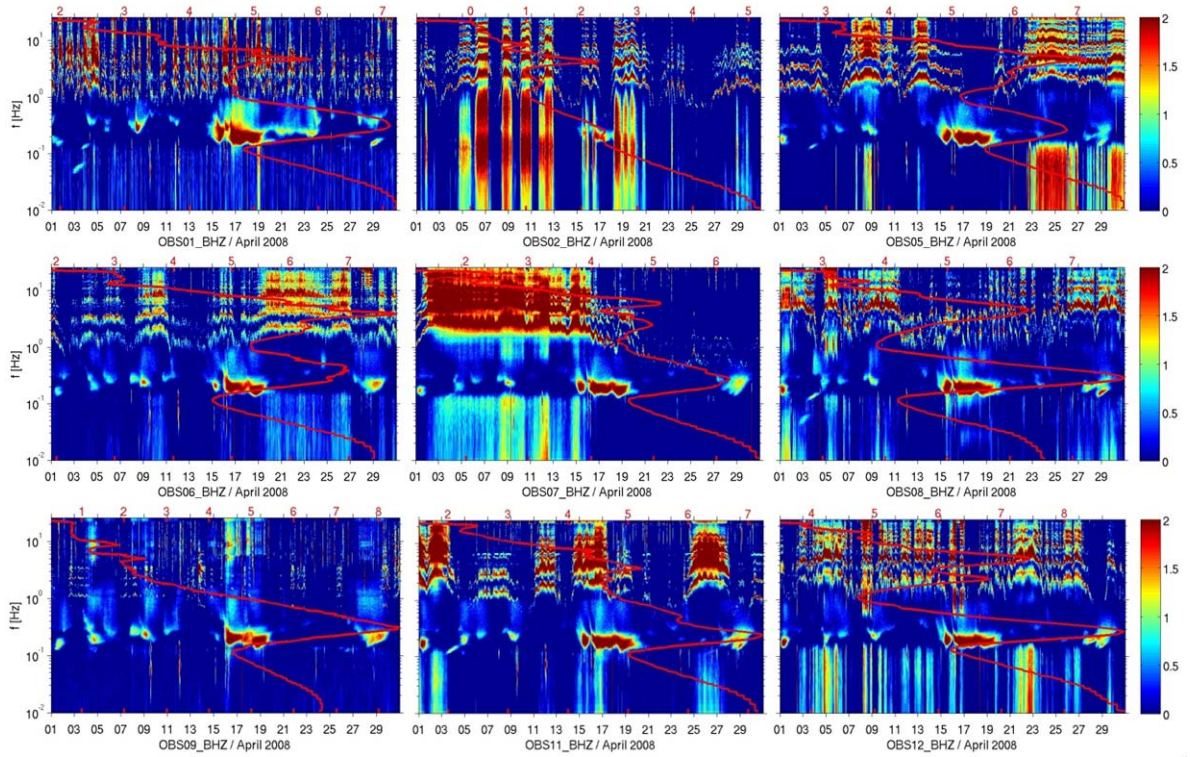

Fig. 6.4.4. Power spectral density plots for the vertical seismic components of the IPY OBS/H stations, for April 2008. The average noise level is shown by the red curve, while the applied color scale expresses positive deviations from the average.

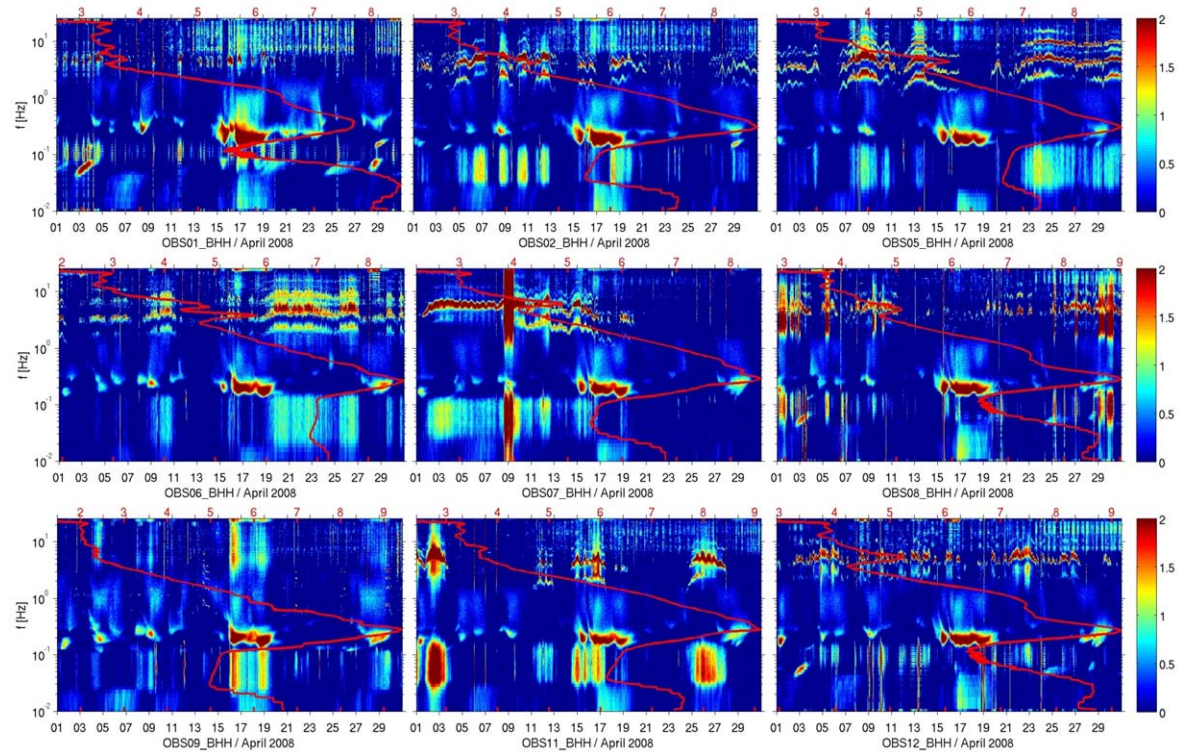

Fig. 6.4.5. As for Fig. 6.4.4, but for the hydrophone channels of the IPY OBS/H stations.

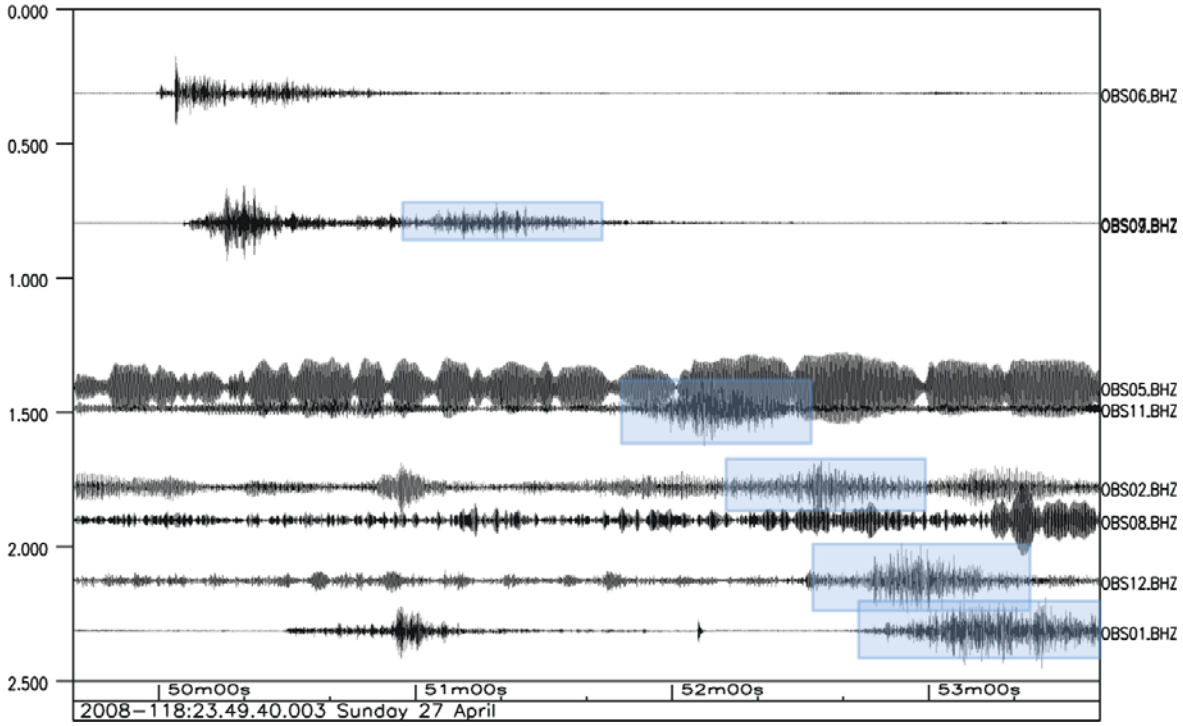

Fig. 6.4.6. Vertical component records on the OBS/H stations of a magnitude 3 event at the Mohns – Knipovich Bend, sorted by epicentral distance. Records are band-pass filtered between 3.5 and 12 Hz. Note that OBS07 and OBS09 are almost at the same distance from the epicenter. High noise conditions at several stations (e.g., OBS05) render picking of body-waves impossible. Colored rectangles enclose T-phases.

6.4.3 Examples of observations

A wide variety of signals was recorded on the seismic and acoustic components of the OBS/H network. There are teleseismic events, stronger regional earthquakes and a huge amount of small, local, seismic events, mostly distributed along the mid-ocean ridge. These can be seen both on the seismic sensors and the hydrophones. An example is shown in Fig. 6.4.7. It is a magnitude 2.6 local event on the Mohns Ridge, recorded on OBS09. It is noteworthy that P-phases appear with quite small amplitudes on all seismic channels, while they are more visible on the hydrophone (BHH). The opposite is true for S-phases, which are in general not well recorded on the pressure sensor, as theoretically expected. Another characteristic feature is the water reflection (Pw), seen on the hydrophone as an impulsive onset. The arrival time difference between the first P-phase onset and the water reflection is 3.9 s, while a water velocity of 1.48 km/s is considered typical for this area (e.g., Ehlers, 2009). This results in a water depth of about 2.9 km, which is in good agreement with our knowledge of the bathymetry in the region.

In addition, several T-phases have been recorded on the hydrophones, but also on the seismometers, mainly from events on the Mohns Ridge. T-phases are observed for events in a minimum distance of about 50 km from the recording station. Their excitation depends strongly on the bathymetry, since bathymetric features act as scatterers, and the effective impedance contrast between the ocean column and the seafloor, (e.g., de Groot-Hedlin and Orcutt, 2001; de Groot-Hedlin, 2004). An example recorded on the seismic sensor is shown in Fig. 6.4.6, where the T-phase, marked with a colored rectangle, can be seen following the body-waves.

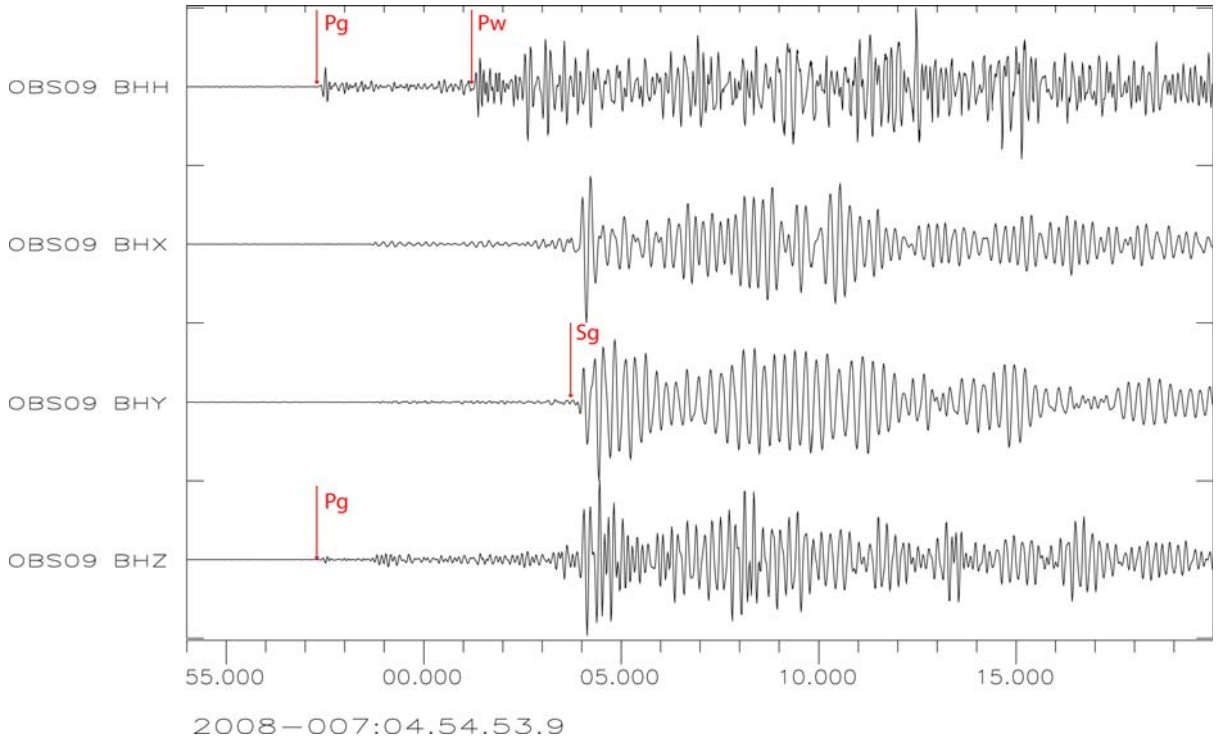

Fig. 6.4.7. Example of a local earthquake on the Mohns Ridge, as recorded on OBS09, band-pass filtered between 3.5 and 12 Hz. The arrivals of the first P-, S- and water-phase are shown. A water velocity of 1.48 km/s for this reflection phase gives a depth of about 2.9 km, which agrees with the bathymetry in this area. Note the rather small amplitudes of the P-phase and the fact that the S-phases cannot be recorded well on the pressure sensor (BHH).

An abundance of hydroacoustic signals was observed on the hydrophones of the IPY network. Among the anthropogenic sources that have been identified in several occasions are airguns (research and industrial), mostly at the southernmost stations closer to the continental shelf. It can be assumed that several signals are associated with boat traffic and marine life, such as whale vocalizations. However, the relatively low sampling rate of the data (50 sps) does not allow a secure identification. Finally, a large part of the recorded hydroacoustic signals remains unclassified.

A different example, shown in Fig. 6.4.8, is a tremor-like signal, consisting of several sub-harmonics, which is mostly visible on the horizontal and vertical components of the seismometer, but is very weak or almost absent on the pressure sensor. The signal is observed at several of the OBS/H, can last for several days and exhibits changes in the resonance frequencies over time. We provisionally interpret this signal as the effect of shear resonances in the upper sediment layers after Godin and Chapman (1999), although its presence at stations where the sedimentary layer is expected to be very thin (e.g., at OBS09) raises some questions on the likelihood of such an interpretation.

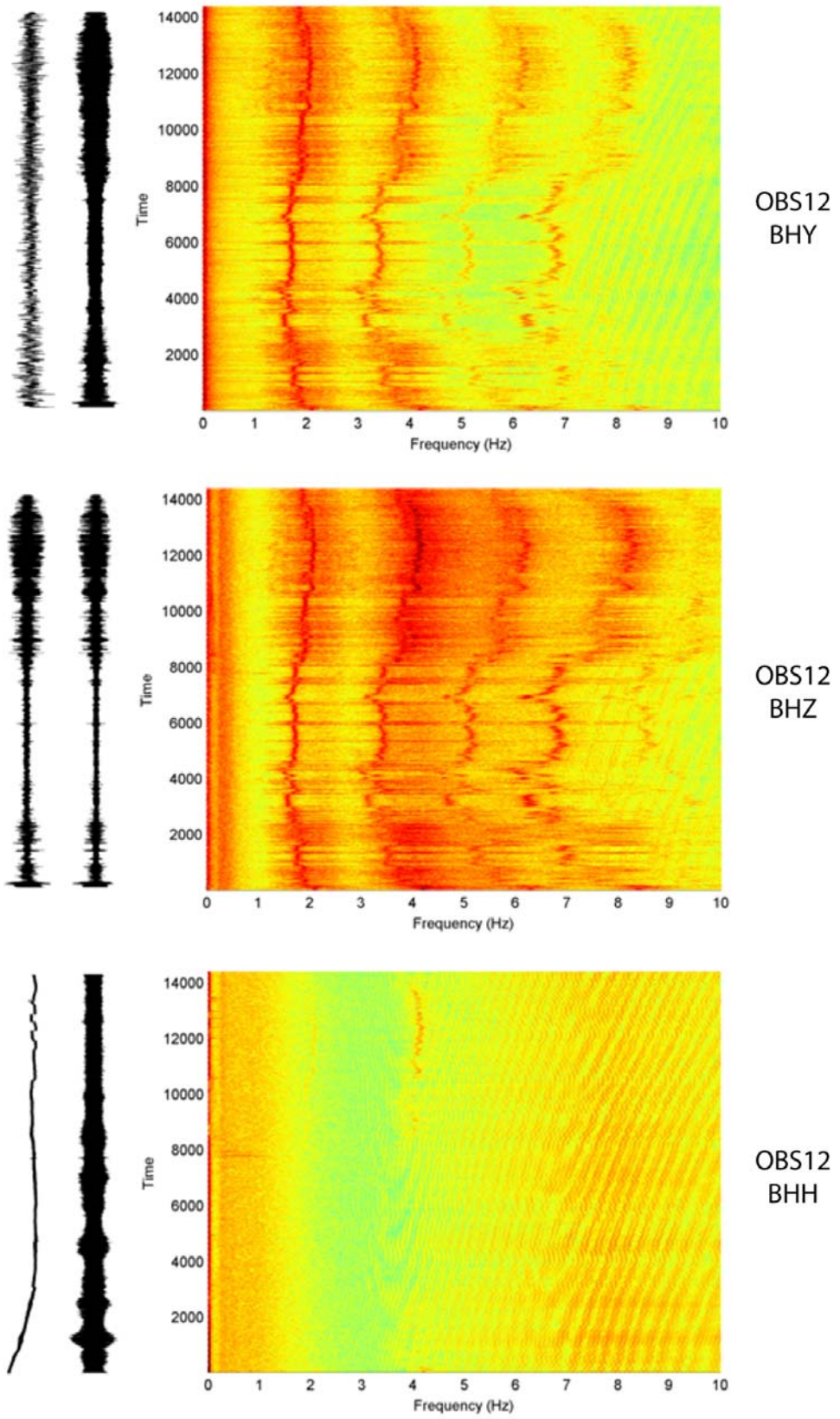

Fig. 6.4.8. Waveforms (left – raw; right – band-pass filtered between 1 and 10 Hz) and corresponding spectrograms up to 10 Hz, for 4 hours of data, on one of the horizontals (BHY), the vertical seismic (BHZ) and the hydrophone channel (BHH) of OBS12.

6.4.4 Location of seismicity

As mentioned in the introduction, the IPY OBS/H network was in operation for almost 11 months, from the end of September 2007 to the end of August 2008. During this time period, a total of 463 earthquakes were located in the wider project area. Our initial knowledge of the seismicity in the region during this time interval came mainly from NORSAR's analyst reviewed bulletin, which contains events with magnitude larger than 2. Its location results for 334 events are shown in Fig. 6.4.9a and reflect the quite large uncertainties introduced by the sparse regional network. Seismicity is mainly observed along the mid-ocean ridge, close to Spitsbergen, and at the sedimentary wedge between the ridge and the continental margin.

All events in NORSAR's bulletin were relocated using in addition all IPY data, as well as any data available from NNSN stations in northern Fennoscandia. The 256 seismic events in the area of Storfjorden, off the east coast of Spitsbergen, belong to the first six months of the aftershock sequence of the 21 February 2008 Mw 6.1 earthquake that was studied by Pirli et al. (2010) and will not be mentioned further herein. In addition to the events in NORSAR's bulletin, the Generalized Beamforming (GBF) algorithm (Ringdal and Kværna, 1989) was reapplied using also the temporary array on Bear Island and results within the project area were relocated manually, using all available data. The same applied for the results of an STA/LTA detector at OBS09 and OBS06, which mostly yielded events at the mid-ocean ridge. Due to the bad noise conditions on most OBS/H stations, power detectors could not be employed on any other ones. The spatial distribution of all (re)located events is shown in Fig. 6.4.9b.

In the relocated dataset, most of the seismicity follows the mid-ocean ridge system, with the largest concentration being observed at the Mohns – Knipovich Bend. Some earthquakes are observed on the sedimentary wedge, but they are fewer compared to the standard NORSAR bulletin results. No special focus will be given herein to the activity located at the southern terminus of the Mohns Ridge and around Jan Mayen, as it is situated outside the project area and lies outside the IPY network. It is however presented for completeness and is included in the statistics that follow.

For the 213 events located along the ridge and on the sedimentary wedge, several trials were performed with different velocity models, in order to define the combination that modeled best the very diverse paths followed by the seismic waves. For instance, stations with a predominantly oceanic path (e.g., JMIC) were modeled using the PREM model (Dziewonski and Anderson, 1981). Specifically for the areas of the sedimentary wedge and the Mohns – Knipovich Bend, the velocity models that provided the best fit to the data were local 1-D averages derived from the three-dimensional Barents3D model (Levshin et al., 2007; Ritzmann et al., 2007). However, even so, events on the sedimentary wedge were not modeled (in terms of velocity model fit) as adequately as events along the ridge, presumably due to the inability of the model to adjust to varying sediment structure. A three-dimensional model is expected to perform much better in this case.

A detailed study of the seismic activity on the sedimentary wedge cannot be achieved without an accurate determination of the hypocenter's location, so that the sediment unit containing the seismic source is identified. The same applies to the seismicity along the ridge, where hypocentral depth constitutes a diagnostic of different processes within the spreading regime. Unfortunately, the resolution achieved by the network was limited and the determination of focal depths was not possible.

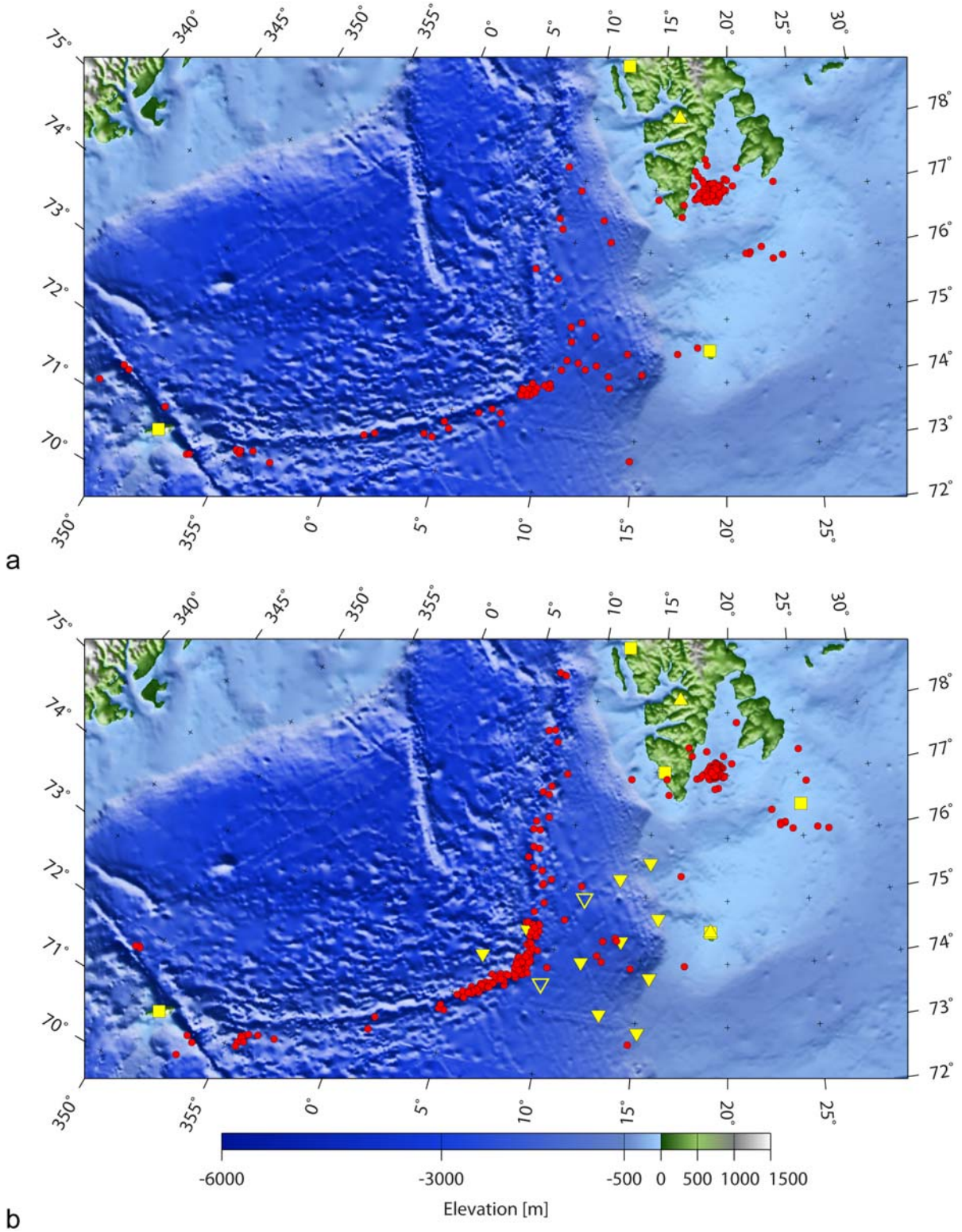

Fig. 6.4.9. a. NORSAR reviewed bulletin solutions for the time interval September 2007 – August 2008. b. Relocated events within the IPY context for the same time interval. The mapped epicenters belong to three different groups: relocations of NORSAR's bulletin solutions, relocations of GBF automatic locations, and locations of events detected on OBS09 and OBS06. Single 3C stations are noted as squares, seismic arrays as triangles and the OBS/H network as inverted triangles (open symbols: no data).

The graphs in Fig. 6.4.10 provide some insight into this problem. Fig. 6.4.10a shows the magnitude distribution for the 78 events (excluding the Storfjorden sequence) in NORSARS's bulletin. Magnitudes are based on amplitude measurements on STA traces for the stations of the permanent regional network. Most earthquakes in this dataset have moderate to small magnitudes, the larger (M > 4.5) ones corresponding to seismicity in the area of Jan Mayen. Fig. 6.4.10b displays the distribution of the number of stations that were actually used to locate the events with the number of events. It becomes clear that more than half of the events were located with a rather small network of 5 stations. This is mostly the effect of the poor SNR on the OBS/H stations, combined with the small magnitude of the events. Fig. 6.4.10c shows the distribution of the minimum epicentral distance in km for the resulting locations. Most of the epicenters are situated at a distance of 50 – 70 km from the nearest station, making the network rather sparse for focal depth determination. Finally, as shown in the rose diagram of Fig. 6.4.10d, there are very few solutions with a primary azimuthal gap less than 100°.

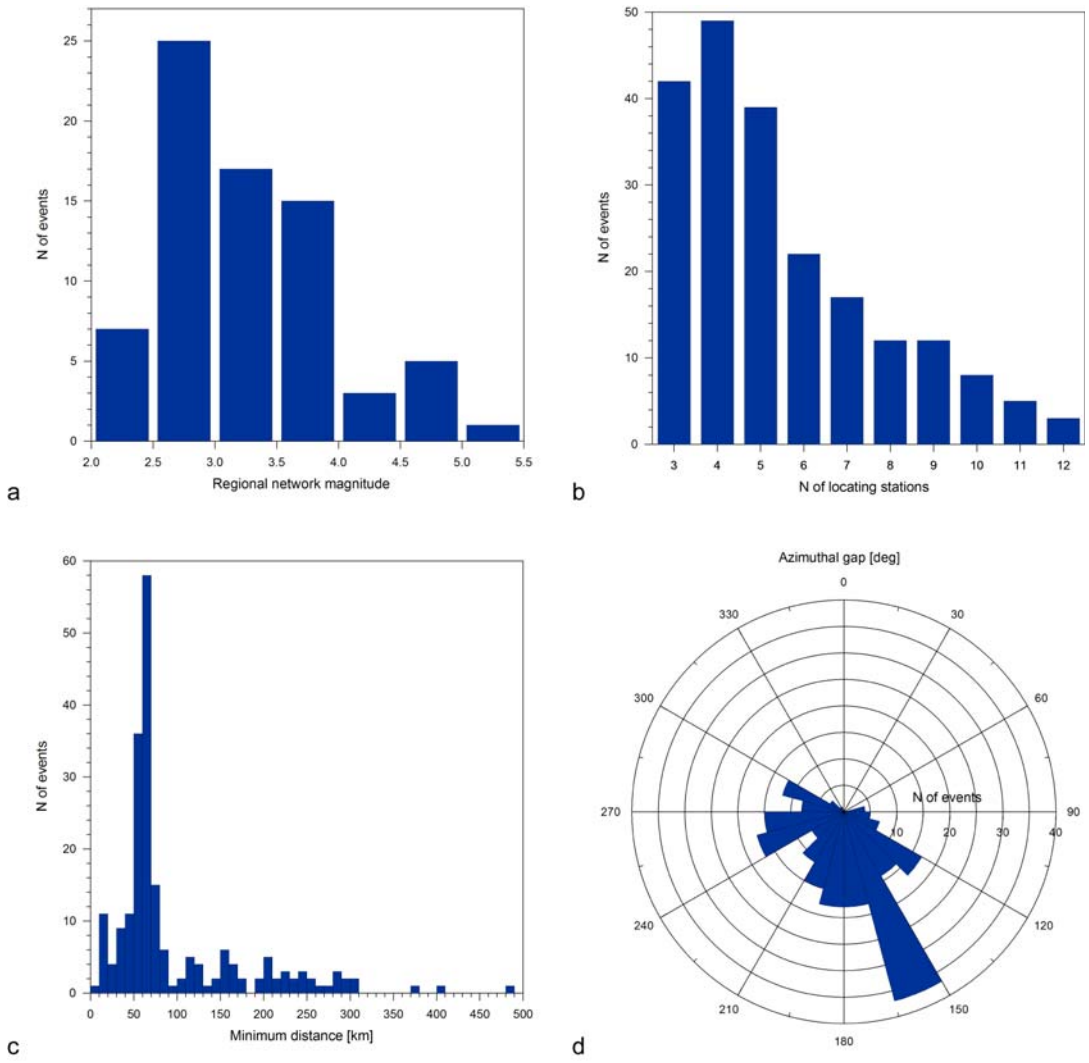

Fig. 6.4.10. a. Histogram of the regional network magnitude distribution for the 78 events in NORSAR's reviewed bulletin. b. Histogram of the number of stations used for location with the number of events for the entire dataset (213 events). c. Histogram of the minimum epicentral distance with the number of events for the entire dataset. d. Rose diagram of the distribution of the primary azimuthal gap in event location for the entire dataset. Intervals of 15° are used.

Despite these shortcomings, the IPY OBS/H network has contributed significantly in enhancing our knowledge of the seismicity in the region. Two examples of event relocation are shown. The first one deals with an event originally located on the Barents shelf, close to Bear Island (2008/01/21 19:31:51, M 3) and the second one with an event on the sedimentary wedge (2008/01/03 21:17:27, M 3), according to NORSAR's reviewed bulletin.

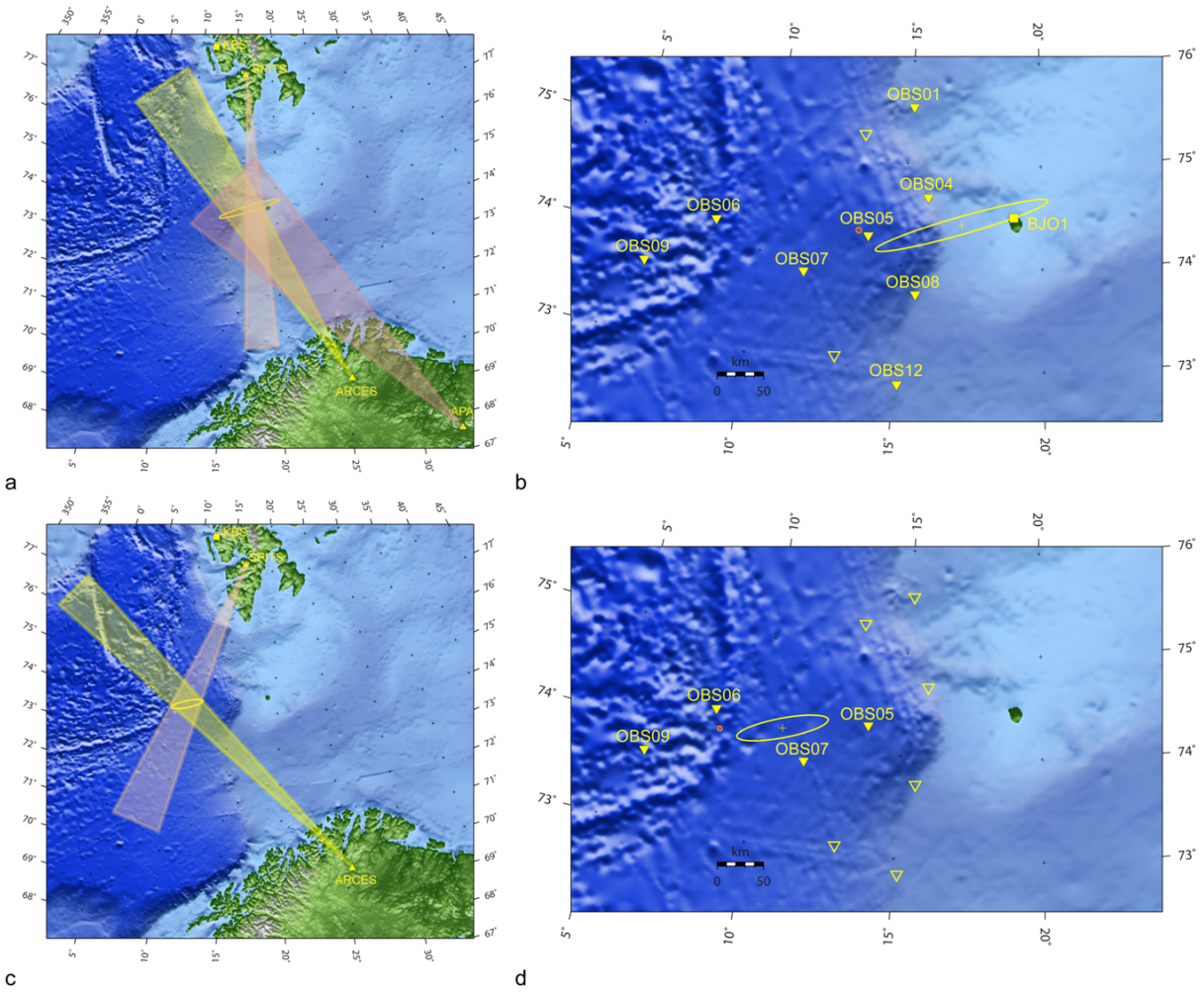

Fig. 6.4.11. a. NORSAR regional reviewed bulletin solution of the 2008/01/21 19:31 M 3 event. Colored triangles denote array backazimuth observations and corresponding uncertainties, while the 90% confidence-level error ellipse is shown in yellow. b. Zoomed-in view of the initial (yellow) and relocated (orange) solutions. The 95% confidence-level error ellipse is calculated for the relocated epicenters. Stations used for the location appear as filled symbols. Seismic arrays are noted as triangles, NNSN stations as squares and IPY stations are inverted triangles. c. Same as a. for the 2008/01/03 21:17 M 3 event. d. Same as b. for the 2008/01/03 21:17 M 3 event. Note the very small dimensions of the relocated error ellipses (in orange) for both events.

The 21 January 2008 earthquake (Fig. 6.4.11a) was located for NORSAR's bulletin using three seismic arrays at regional distances (ARCES, APA and SPITS) and station KBS. The location result is dominated by the backazimuth observations from the three arrays and their corresponding uncertainties (colored triangles in Fig. 6.4.11a,c). Relocating the event using in addition the OBS/H network, BJO1, HSPB and HOPEN results in the epicenter moving approximately 130 km westwards, on the sedimentary wedge (Fig. 6.4.11b). In fact, the intro-

duction of P- and S-phase readings from BJO1 is enough to move the epicenter off the continental shelf, but the addition of the OBS/H stations (8 out of 10 could be used in this case, with a minimum epicentral distance of 12 km from OBS05) refines the solution. The 3 January 2008 event (Fig. 6.4.11c) was located for NORSAR's bulletin near the end of the sedimentary wedge and close to the southern end of the Knipovich Ridge, using two seismic arrays (SPITS and ARCES) and station KBS. It was relocated using in addition OBS06, OBS09, OBS07 and OBS05, the epicenter moving to the mid-ocean ridge (Fig. 6.4.11d).

These two examples illustrate clearly the significance of the IPY network to the connection of located events with the correct geodynamic environment. The relocated seismicity in Fig. 6.4.9b is not only more populous, compared to the listings of NORSAR's reviewed bulletin, but the geographic spread is significantly less and seismic events are better associated with their corresponding geodynamic sources. Thus, sedimentary wedge seismicity has noticeably decreased, compared to the impression given by the bulletin, since several events are now correctly attributed to the mid-ocean ridge system. It should be noted that it cannot be expected that routine analysis results can be used for a seismotectonic or geodynamic study, especially in such cases, where seismicity is remote, in an offshore area that is covered only by a very sparse, regional network. However, this highlights the importance of temporary deployments to provide, even for limited time intervals, a more accurate image of the spatiotemporal distribution of the seismic activity for a given region.

6.4.5 Conclusions

We presented the contribution of the IPY OBS/H network to the study of the seismicity at the wider region of the western Barents Sea continental margin. Some equipment and data loss took place within the experiment, but most of the stations of the deployment contributed seismic and pressure data for approximately 11 months.

A variety of seismic and acoustic signals were recorded during the project; they included seismicity from different epicentral distance ranges and geodynamic environments, hydroacoustic phases, signals from anthropogenic sources (e.g., airgun shots, boat traffic), weather related phenomena, ocean currents, as well as many unclassified signals. In general, the noise level among the OBS/H stations was rather high, imposing restrictions to the analysis of seismic data. The two deepest stations (OBS09 and OBS06) were the ones with the best SNR, and therefore a strong focus was put on the exploitation of their data.

Unfortunately, the network did not achieve the required resolution to allow the determination of focal depth for the events along the mid-ocean ridge and the sedimentary wedge, which was one of the aims of the project. However, and despite all difficulties, the network had a significant contribution to the monitoring and location of the seismic activity in the region. Comparisons of our knowledge of the seismicity only with the use of the permanent, regional network, and with the use of the IPY stations, show not only a quantitative increase in the number of located events, but a clearly enhanced resolution. This is particularly important for such remote, offshore areas, since it allows us, even if it is only for a relatively short time interval, to obtain accurate images of the spatiotemporal distribution of the seismic activity.

Acknowledgements

The power spectral density plots of Figs. 6.4.4 and 6.4.5 were prepared by Michael Roth. The project "The Dynamic Continental Margin Between the Mid-Atlantic-Ridge System (Mohns Ridge, Knipovich Ridge) and Bear Island" was part of the Norwegian contribution to the International Polar Year 2007-2008 activities organized by the Norwegian IPY Committee and mainly financed by the Norwegian Research Council (Contract Number 176069/S30).

Myrto Pirli
Johannes Schweitzer
The IPY Project Consortium

References

Cirrus Logic (2010): Crystal CS5378 Low-Power Single-Channel Decimation Filter. CS5378_F3.pdf, Cirrus Logic Inc., Austin, Texas, 88 pp.

de Groot-Hedlin, C. & J.A. Orcutt (2001): Excitation of T-phases by seafloor scattering. J. Acoust. Soc. Am., **109(5)**, 1944-1954.

de Groot-Hedlin, C. (2004): Criteria for discretization of seafloor bathymetry when using a stairstep approximation: Application to computation of T-phase seismograms. J. Acoust. Soc. Am., **115(3)**, 1103-1113.

Dziewonski, A.M. & D.L. Anderson (1981): Preliminary reference Earth model. Phys. Earth Planet. Interiors, **25**, 297-356.

Ehlers, B.-M. (2009): A geodynamic model of the northern North Atlantic. PhD Thesis, Alfred Wegener Institute for Polar and Marine Research, Bremerhaven, Jacobs University Bremen, Bremen, 228 pp.

Godin, O.A. & D.M.F. Chapman (1999): Shear-speed gradients and ocean seismo-acoustic noise resonances. J. Acoust. Soc. Am., **106(5)**, 2367-2382.

High Tech, Inc. (2005): HTI-01-PCA/ULF Hydrophones 31205605 – 31208505. High Tech, Inc., Gulfport, Mississippi, 4 pp.

Levshin, A., J. Schweitzer, Ch. Weidle, N. Shapiro & M. Ritzwoller (2007): Surface wave tomography of the Barents Sea and surrounding regions. Geophys. J. Int., **170**, 441-459.

Pirli, M., J. Schweitzer, L. Ottemöller, M. Raeesi, R. Mjelde, K. Atakan, A. Guterch, S.J. Gibbons, B. Paulsen, W. Dębski, P. Wiejacz & T. Kværna (2010): Preliminary analysis of the 21 February 2008, Svalbard (Norway), seismic sequence. Seism. Res. Lett., **81(1)**, doi:10.1785/gssrl.81.1.50.

Ringdal, F. & T. Kværna (1989): A multichannel processing approach to real time network detection, phase association and threshold monitoring. Bull. Seism. Soc. Am., **79**, 1927-1940.

Ritzmann, O., N. Maercklin, J. I. Faleide, H. Bungum, W. D. Mooney & S. T. Detweiler (2007): A 3D geophysical model for the crust in the greater Barents Sea region: Database compilation, model construction and basement characterisation. Geophys. J. Int., **170**, 417-435.

Schweitzer, J. & the IPY Project Consortium Members (2008): The International Polar Year 2007-2008 Project "The Dynamic Continental Margin between the Mid-Atlantic-Ridge System (Mohns Ridge, Knipovich Ridge) and the Bear Island Region". NORSAR Scientific Report, **1-2008**, 53-63.

SEND GmbH (2007): Application Note: Geolon-MCS Digital Filtering. Digital_filtering_mcs.doc, SEND GmbH, Hamburg, Germany, 8 pp.

SEND GmbH (2009): GEOLON-MCS Marine Compact Seismocorder, User Manual. MCS1.09.mnl.doc, SEND GmbH, Hamburg, Germany, 38 pp.

Wenz, G.M. (1962): Acoustic ambient noise in the ocean: spectra and sources. J. Acoust. Soc. Am., **34(12)**, 1936-1956.